Article:

Zhang, W., Chen, J., Luo, X. et al. (2017) Modelling and process analysis of post-combustion carbon capture with the blend of 2-amino-2-methyl-1-propanol and piperazine. International Journal of Greenhouse Gas Control, 63. pp. 37-46. ISSN: 1750-5836

https://doi.org/10.1016/j.ijggc.2017.04.018

Modelling and Process Analysis of Post-combustion Carbon Capture with a Novel Solvent of the blend of 2-amino-2-methyl-1-propanol (AMP) and Piperazine (PZ)

Weiyu Zhang[a], Jian Chen[a,*], Xiaobo Luo[b], Meihong Wang[b]

[a]*State Key Laboratory of Chemical Engineering, Tsinghua University, Beijing 100084, China*

[b]*Department of Chemical and Biological Engineering, School of Engineering, The University of Sheffield, S10 2TN, UK*

[*]*Corresponding author 1. Tel: +86 10 62798627; Fax: +86 10 62770304; Email:* cj-dce@tsinghua.edu.cn

Abstract

Recent pilot plant experiments have proved that a novel solvent blend of 2-amino-2-methyl-1-propanol (AMP) and piperazine (PZ) has better performance in energy saving than the traditional solvent monoethanolamine (MEA) for chemical absorption CO_2 capture process. This paper presented the systemic study on modeling and process analysis of the CO_2 capture process with an AMP+PZ aqueous solvent using Aspen Plus® software. A rate-based steady state process model was developed by updating the thermodynamic model and chemistry reactions with kinetic parameters of the AMP-PZ-H_2O-CO_2 system. The process model was validated with the experimental data and the results showed an excellent agreement. The process model was then scaled up to match the capacity of an industrial scale coal-fired power plant. A parametric study of the industrial scale model shows that the reboiler duty would be reduced upon lowering the CO_2 removal rate, increasing the ratio of AMP in the solvent, and increasing the stripper pressure. Process configuration modifications, including intercooled absorber (ICA), lean vapor compressor (LVC) and rich solvent split (RSS), have been implemented and the energy demand were reduced by 6.7%, 2.7%, and 8.5% accordingly. The combination of ICA+LVC, ICA+RSS, and RSS+LVC modifications obtained an energy saving of 8.5%, 14%, and 9.3% respectively. The combination of ICA +RSS+LVC reduced the energy demand by 15.2%.

Key words: CO_2 capture, rate-based model, process modification, regeneration energy, novel solvent

---

1. **Introduction**

As a major greenhouse gas produced by human activities, CO_2 atmosphere concentration is currently 40% higher than it was when industrialization began (NOAA, 2015). Anthropogenic CO_2 emission contributes 64% of man-made global warming (). Therefore, reduction of greenhouse gas emissions is essential for limiting the global temperature increase. Chemical absorption of CO_2 is the most widely applied process for CO_2 capture from flue gas (Wang et al., 2011). However, the traditional solvent, MEA, has some drawbacks like thermal and oxidative degradation and a large energy demand for solvent regeneration (Luo et al., 2015; Rochelle, 2009). To make the CO_2 capture process economically viable, seeking highly effective solvents and optimizing the process flowsheet are two main paths to reducing the energy requirement.

One novel solvent is a blend of 2-amino-2-methyl-1-propanol (AMP) and piperazine (PZ). AMP has a higher CO_2 absorption capacity than MEA due to its sterically hindered character that reduces the stability of the formed carbamate. AMP can absorb up to one mole of CO_2 per mole of amine while MEA can absorb only half a mole of CO_2 per mole of amine (Chowdhury et al., 2011). The regeneration energy requirement is lower as well. However, AMP has a relatively low rate of CO_2 absorption (Bavbek and Alper, 1999). PZ is used as an activator or promoter added to AMP to increase the chemical reaction rate, and thus the mass transfer rate. The reaction between CO_2 and PZ is rapid due to the cyclic diamine structure, and the reaction is almost 10 times faster than the one between CO_2 and MEA (Bishnoi and Rochelle, 2000). Freeman (Freeman et al., 2010b) reported the rate of CO_2 absorption into 8 M PZ is 1.5–3 times that of 7 M MEA. In summary, the AMP+PZ blend could utilize the CO_2 capacity of AMP and elevate the reaction rate while retaining low regeneration energy. Brúder (Brúder et al., 2011) reported experimental tests for AMP/PZ (3/1.5 M) and for 30 wt% MEA systems. The AMP/PZ system has ~128% higher specific cyclic capacity when operating between 40 and 80°C and almost twice the CO_2 partial pressure at 120°C compared to MEA.

This blend solvent is also more resistant to thermal and oxidative degradation according to open literature. Lepaumier (Lepaumier et al., 2009) examined the oxidative degradation of 12 ethanolamines and ethylenediamines, and reported that AMP has the lowest degradation rate and is more resistant to oxidation than MEA. In Freeman's study (Freeman et al., 2010a), PZ was observed to be an effective resistant to oxygen and thermal degradation up to a temperature up to 150°C. As for solubility, Both AMP and PZ are miscible with water. For AMP-PZ-CO2 system, Brúder (Brúder et al., 2010) tested different concentrations of AMP/PZ with high CO2 concentration to avoid forming precipitates. For the blend of 3M AMP + 2M PZ (28 wt% AMP + 17 wt% PZ), it was observed that all crystals dissolved at 22 °C if mixed, which suggested this system will not make problems in a stable industrial operation.

The AMP+PZ blend solvent has been applied in pilot plant experimental studies around the world. Śpiewak (Śpiewak et al., 2015) conducted process development unit scale (PDU-scale) experiments, which is a more reliable representation of the actual industrial process, for CO_2 removal from a gas mixture by the application of aqueous solutions of MEA and AMP promoted with PZ. The results showed that using an AMP/PZ mixture enables a reduction of the solvent heat duty. Artanto (Artanto et al., 2014) evaluated the pilot-scale performance of an aqueous mixture of 25 wt% AMP and 5 wt% PZ compared with the baseline performance of aqueous 30 wt% MEA. The effects of liquid/gas (L/G) ratio and lean solvent loading on CO_2

recovery and reboiler heat duty were studied and the results showed that the AMP/PZ mixture is a promising alternative to MEA. Knudsen (Knudsen et al., 2011) showed that CESAR 1 (28 wt% AMP + 17 wt% PZ) provided a substantial decrease in the regeneration energy requirement as well as the required solvent circulation rate compared to 30% MEA. Process modifications like absorber inter-cooling were installed, resulting in ~25% saving in the regeneration energy compared to that of the standard MEA process (3.7 GJ/ton CO_2), realized with the CESAR 1 solvent. Mangalapally (Mangalapally and Hasse, 2011a) presented a pilot plant study of the CO_2 capture process using CESAR 1 and MEA. For each solvent and a constant CO_2 removal rate of 90%, the minimum regeneration energy was determined for an optimal solvent flow rate. Reductions of ~20% in the regeneration energy and 45% in the solvent flow rate were reported.

Experimental and theoretical investigations of the CO_2 absorption in PZ-activated concentrated aqueous AMP are presented by Samanta (Samanta and Bandyopadhyay, 2009) and Dash (Dash et al., 2011). The CO_2 absorption into the aqueous amine solutions has been described by a combined mass transfer-reaction kinetics-equilibrium mode, developed according to Higbie's penetration theory. A rigorous thermodynamic model in Aspen Plus was developed by Li (Li et al., 2014) to predict the thermodynamic properties of PZ–AMP–CO_2–H_2O over a wide range of conditions using the electrolyte non-random two-liquid activity coefficient (e-NRTL) model and Redlich–Kwong (RK) equation. This model succeeded in predicting CO_2 solubility, nuclear magnetic resonance (NMR) speciation, and heat of CO_2 absorption for AMP+PZ blends with variable loadings and temperatures, which could be used for the simulation and design of the CO_2 capture process. As for simulation work, only Dash (Dash et al., 2014) presented a simulation study of the CO_2 capture process using an aqueous blend of AMP+PZ solvents. Using the absorption-regeneration process, the CO_2 capture from the flue gas of a coal-fired power plant and parametric studies have been simulated with RadFrac-RateSep block in Aspen Plus. However, the simulation of a commercial-scale model and process modifications for AMP+PZ has not yet been reported.

Consequently, in this study, a full-scale model of CO_2 capture with an AMP+PZ blend solvent was developed and used for studies focusing on reducing the solvent regeneration heat. The effects of different process parameters on the reboiler duty were investigated, and process modifications were applied to further reduce the energy consumption.

2. Model development

2.1. Pilot scale model development in Aspen Plus®

In order to successfully simulate the CO_2 absorption process, a thermodynamic model, a chemistry model, reaction kinetics, and transport property models were implemented in Aspen Plus. The e-NRTL-RK method was chosen and the thermodynamic model developed by Li (Li et al., 2014) was used to calculate the thermodynamic properties of components in the simulation. The heat capacity and coefficients for the Antoine's equation for AMP, the NRTL binary parameters (molecular-molecular), and the e-NRTL parameters (molecular-electrolyte) were used from the regressed results of this model. Henry's constants, dielectric constants, and other data were obtained from the Aspen Plus data bank. In addition, the ion components were user-defined and their physical properties, including the aqueous-phase Gibbs free energy and heat of formation at infinite dilution and 25 °C and heat capacity at infinite dilution, were taken from the work of Li (Li et al., 2014).

As for the chemistry model, AMP is considered to associate with H_3O^+ to form the ion $AMPH^+$ and to react with CO_2 to from an unstable carbamate. This carbamate easily reacts with other species in aqueous solution to regenerate $AMPH^+$. PZ is considered to associate with H_3O^+ to form PZH^+ and also react with CO_2 to form the carbamate $PZCOO^-$ and the di-carbamate $PZ(COO^-)_2$. Therefore, the following electrolyte solution chemical reactions, all of which are assumed to reach chemical equilibrium, were modeled as the global electrolyte calculation option in the simulation.

$$\mathrm{H_2O} \leftrightarrow \mathrm{H^+} + \mathrm{OH^-} \tag{1}$$

$$\mathrm{CO_{2(aqueous)}} + \mathrm{H_2O} \leftrightarrow \mathrm{H^+} + \mathrm{HCO_3^-} \tag{2}$$

$$\mathrm{HCO_3^-} \leftrightarrow \mathrm{H^+} + \mathrm{CO_3^{2-}} \tag{3}$$

$$\mathrm{PZH^+} \leftrightarrow \mathrm{PZ} + \mathrm{H^+} \tag{4}$$

$$\mathrm{PZH^+} \leftrightarrow \mathrm{PZ} + \mathrm{H^+} \tag{5}$$

$$\mathrm{PZ} + \mathrm{HCO_3^-} \longleftrightarrow \mathrm{PZCOO^-} + \mathrm{H_2O} \tag{6}$$

$$\mathrm{PZCOO^-} + \mathrm{HCO_3^-} \longleftrightarrow \mathrm{PZ(COO^-)_2} + \mathrm{H_2O} \tag{7}$$

$$\mathrm{HPZCOO} \longleftrightarrow \mathrm{PZCOO^-} + \mathrm{H^+} \tag{8}$$

$$\mathrm{AMP} + \mathrm{H^+} \longleftrightarrow \mathrm{AMPH^+} \tag{9}$$

The equilibrium constants were calculated from the standard Gibbs free energy change which can~~could~~ be determined by the properties of the ions.

$$K_j = \exp(-\frac{\Delta G_j^0}{RT}) \tag{10}$$

where K_j is the chemical equilibrium constant of reaction j, ΔG_j is the change of reference state free energies for reaction j, R is the universal gas constant, and T is the temperature.

For the rate-based simulation, reaction kinetics are required; therefore, a reaction model is created, in which all reactions are assumed to be at equilibrium, except those of CO_2 with base in the solution. The power law expressions are used for the rate-controlled reactions.

$$r = k_0 \exp(\frac{-E}{R}\left(\frac{1}{T} - \frac{1}{298}\right)) \prod_{i=1}^{n} C_i^{a_i} \tag{11}$$

where r is the rate constant, k_0 is the pre-exponential factor, E is activation energy, R is gas law constant, C is concentration in molarity, and T is the temperature.

The kinetic parameters used in this model were taken from literature and presented in Table 1.

Table 1. Kinetic parameters

	k_0	E/cal/mol	Reference
$\mathrm{CO_2} + \mathrm{OH^-} \rightarrow \mathrm{HCO_3^-}$	4.23E13	13245	(Pinsent et al., 1956)
$\mathrm{HCO_3^-} \rightarrow \mathrm{CO_2} + \mathrm{OH^-}$	2.38E17	29451	(Pinsent et al., 1956)~~?~~
$\mathrm{PZ} + \mathrm{CO_2} + \mathrm{H_2O} \rightarrow \mathrm{PZCOO^-} + \mathrm{H_3O^+}$	5.8E4	35000	(Bishnoi and Rochelle, 2002)

$PZCOO^- + H_3O^+ \rightarrow PZ + CO_2 + H_2O$	3.62E10	8038	(Bishnoi and Rochelle, 2002)?
$PZCOO^- + CO_2 + H_2O \rightarrow PZ(COO^-)_2 + H_3O^+$	5.56E25	18372	(Samanta and Bandyopadhyay, 2009)
$PZ(COO^-)_2 + H_3O^+ \rightarrow PZCOO^- + CO_2 + H_2O$	5.95E4	35500	(Samanta and Bandyopadhyay, 2009)?
$AMP + H_2O + CO_2 \rightarrow HCO_3^- + AMPH^+$	1.943E10	43000	(Saha et al., 1995)

In this study, the simulation approach including feed stream conditions and unit operation block specifications were based on the pilot plant study by Mangalapally (Mangalapally and Hasse, 2011b). The typical flow sheet for the CO_2 capture process is shown in Figure 1**Error! Reference source not found.**. The feed streams are the pre-treated flue gas, consisting of CO_2, N_2 and H_2O, and the lean solvent, containing aqueous AMP+PZ solution loaded with a small amount CO_2. The feed specifications were set as the experiment data. The flue gas was fed into the bottom of the absorber while the lean amine solvent entered the top. CO_2 in the flue gas was chemically absorbed and the treated gas exited from the top of the absorber. The rich solvent loaded with CO_2 left from the bottom and was pumped into the lean-rich cross heat exchanger. The pressure increase was 1 atm. The lean-rich heat exchanger was modeled with Aspen HeatX. The calculation type was shortcut, and the hot outlet-cold inlet temperature difference was set to 10 °C. The cold rich stream exchanged heat with the hot lean stream from the reboiler and then was introduced into the top of the stripper. The rich solvent flowed down and contacted with the vapor generated from the reboiler. The reaction of CO_2 and amine reverses due to the temperature and pressure conditions in the stripper, and a concentrated CO_2 stream was obtained at the top. To reduce solvent loss, the CO_2 stream entered a flash tank and the liquid reflux was returned to the top of the stripper.

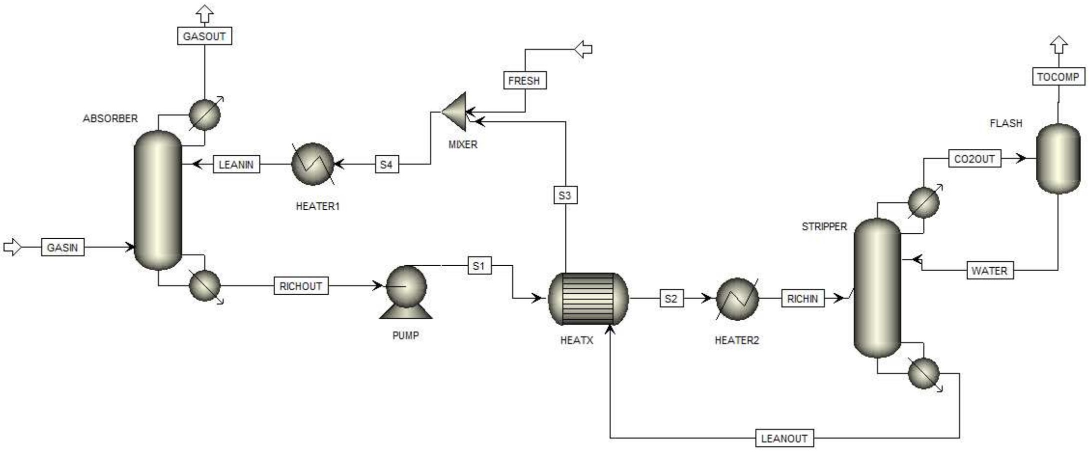

The hot lean solvent was cooled by the heat exchanger and a cooler to reach the temperature of the absorber, and it then traveled back to the absorber.

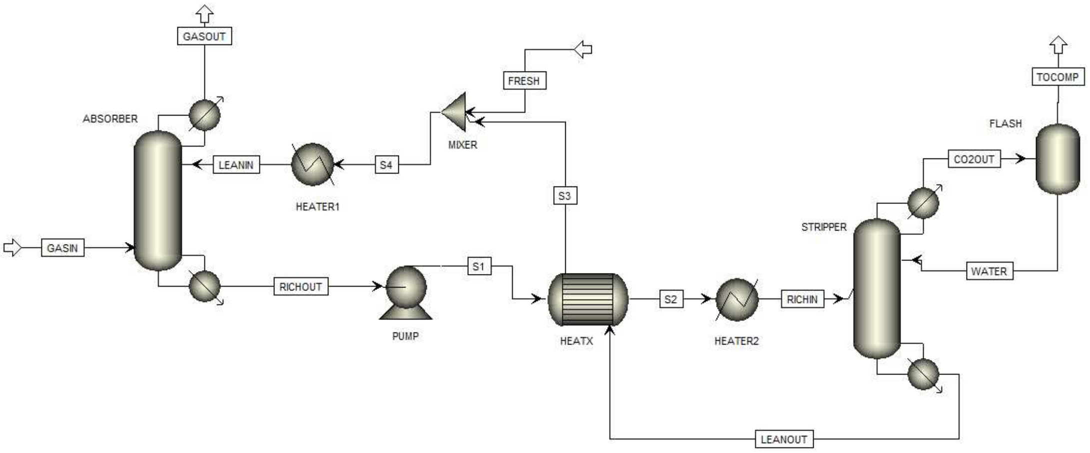

Figure 1.~~.~~ Process flowsheet for the CO_2 capture process.

The absorber and stripper were modeled with RadFrac and the rate-based calculation type was chosen. This rate-based model, used for multistage separation operations, is rigorous and offers higher model fidelity over the traditional equilibrium-stage modeling approach (Taylor et al., 2003). It provides excellent capability, and the simulation results were in good agreement with reported experimental data (Niu et al., 2012; Zhang et al., 2009). Standard BX structured packing sections were used for both columns. The section diameter was 0.125 m for both columns, and the packing height was 4.25 m and 2.55 m for the absorber and stripper, respectively. The model allows several options for modeling film resistance. The film discretization option was set for liquid film, and the number of discretization points was 5. The mass and heat transfer coefficient method, as well as the holdup correlation, were both determined according to the literature and by the accuracy of the simulation results. The main specifications used for the two columns are presented in Table 2.

Table 2. Specifications for absorber and stripper

	ABSORBER(Radfrac)	STRIPPER(Radfrac)
Calculation type	Rate-Based	Rate-Based
Stages	11	9
Condenser	None	Partial vapor
Reboiler	None	Kettle reboiler
Packing	STANDARD BX by Sulzer	STANDARD BX by Sulzer
Section diameter	0.125 m	0.125 m
Section packed height	4.25 m	2.55 m
Mass transfer coefficient method	Bravo et al. (1985)	Bravo et al. (1985)

Interfacial area method	Bravo et al. (1985)	Bravo et al. (1985)
Heat transfer coefficient method	Chilton and Colburn	Chilton and Colburn
Holdup correlation	Bravo et al. (1992)	Bravo et al. (1992)
Film resistance options	Discrxn for liquid ; Film for vapor	Discrxn for liquid; Film for vapor
Additional discretization points for liquid film	5	5

2.2. **Validation with pilot plant data**

Mangalapally (Mangalapally and Hasse, 2011b) conducted a systematic pilot plant study of the CO_2 capture process with a blend solvent (28 wt% AMP+17 wt% PZ+55 wt% H2O). The measurements are performed at a constant CO_2 removal rate of 90% by adjusting the regeneration energy in the desorber for systematically varied solvent flow rates. Therefore, the detailed lean and rich loading, the reboiler duty, and the CO_2 mass flow captured were reported and compared with the simulation results. Some of the most representative data are presented in Table 3. In these cases, the lean loading was fixed while the experimental data and other simulation results were compared. The largest relative error was ~5%, which suggests that this model can predict with precision.

Table 3. Simulation results validated with experimental data

	L/G=1.25			L/G=1.9			L/G=2.9		
	pilot plant	simulation	Relative Error	pilot plant	simulation	Relative Error	pilot plant	simulation	Relative Error
Lean loading (mol CO_2/kg solvent)	0.3	0.30	/	0.8	0.80	/	1.1	1.10	/
Rich loading (mol CO_2/kg solvent)	2.7	2.57	4.8	2.4	2.30	4.2	2.1	2.03	3.3
CO_2 mass flow captured (kg/h)	10.5	10.01	4.7	10.5	10.21	2.8	10.5	10.45	0.5
CO_2 removal rate%	90	86.3	4.1	90	88.0	2.2	90	90.1	0.1
Rebolier duty(GJ/ton)	3.3	3.47	5.2	3.5	3.62	3.4	4.0	3.80	5.0

2.3. **Scale-up**

The CO_2 capture process can be used at a commercial-scale power plant. While the model has been validated at a pilot plant scale, it is necessary to scale it up to match the capacity of a 660-MW_e coal-fired power plant and to study the performance. The methodology described by Sinnott (Sinnott and Towler, 2013) on CO_2 capture process has been adapted by several researchers. Based on the work of Hanak (Hanak et al., 2014), the conditions of the flue gas and the initial specifications required for scale-up are given in Table 4.

Table 4. Initial specification required for scale-up

Parameter	Value
Flue gas composition (mol%)	CO_2: 15, N_2: 77, H_2O: 8
Flow rate of flue gas (kg/s)	635.2

Mass fraction of CO_2 in the flue gas	0.2217
Temperature of flue gas (°C)	40
Recovered CO_2 flow rate (kg/s)	133.4
First guess L/G ratio	1.25

A first-guess column diameter, which is also an initial input for Aspen Plus simulation, was determined from the generalized pressure-drop correlation.

$$F_{LV} = \frac{L_w^*}{V_w^*}\sqrt{\frac{\rho_V}{\rho_L}} \tag{12}$$

$$K_4 = \frac{13.1(V_w^*)^2 \cdot F_p \cdot (\mu_L/\rho_L)^{0.1}}{\rho_V(\rho_L - \rho_V)} \tag{13}$$

As expressed in the equations, F_{LV} is a flow parameter dependent on the L/G ratio of the column while K_4 is a modified gas load. Sinnott (Sinnott and Towler, 2013) also recommended the pressure drop per meter packing for absorbers and strippers to be 15–50 mm of water per meter of packing height. Consequently, 42 mm is chosen in the design of both of the columns in order to operate at the best economical pressure drop. F_{LV} can be determined from the specification of flue gas and lean solvent. K_4 can be obtained from Fig. 11.46 in Sinnott and Towler, 2013. V^*_w, the vapor mass flow rate per unit cross-sectional area, is calculated from the value of K_4, and the total cross-sectional area can be obtained from the flue gas flow rate. Since the total cross-sectional area has been determined, the diameter of the two columns can be set. The initial guess input is then simulated and adjusted to avoid the column flooding exceeding 80%. The specification of packing is the same as that in the pilot scale simulation. The scale-up results of the absorber and the stripper are shown in 5. For the absorber, a column with a diameter of 20.8 m is chosen, while a column with a diameter of 12.0 m is selected for the stripper.

Table 5. Scale-up results of the absorber and the stripper

	ABSORBER (Radfrac)	STRIPPER (Radfrac)
Section diameter(m)	20.8 m	12.1 m
Section packed height(m)	30 m	30 m
Lean solvents flow rate(kg/s)	2722.95	/
Reboiler duty (GJ/ton CO_2)	/	5

3. Parametric study

The thermal energy consumption is expected to be a major contributor to the energy penalty, and a reduction in the energy required will give a significant saving on the total cost. Consequently, in this study the reboiler duty is set as the target function. The heat provided in the reboiler is the sum of the heat of water vaporization, the heat of CO_2 desorption, and the sensible heat required to bring the solvent to reboiler temperature (Freguia and Rochelle, 2003). A set of process conditions could affect one or more of these three parts, leading to a change in the reboiler duty.

In this study, key process parameters of the base case are presented in Table 6. The following parameters were chosen to be varied: the amount of CO_2 removed (50–90% removal), the PZ concentration in a total 45 wt% solvent (7–22 wt% PZ), the L/G ratio (1.5-4.5) and the stripper pressure (0.8–3 atm).

Table 6. Simulation results for the baseline case

Parameter	Value
Solvent concentration	28 wt% AMP + 17 wt% PZ
CO_2 removal rate	90%
Solvent mass flow rate (kg/s)	1344.40
Liquid to gas ratio (mass basis)	2.12
Lean loading (mol/mol)	0.133
Rich loading (mol/mol)	0.565
Reboiler duty (GJ/ton CO_2)	3.18

The full-scale model of CO_2 capture process is used to study the effect of operation parameters on the reboiler duty. For each case, the flue gas flow rate and the composition remain unchanged. The CO_2 removal rate is set as a design specification. The lean loading, representing the degree of solvent regeneration, is calculated as the reboiler energy input is changed. Once the lean loading has been determined, the solvent flow rate is then varied to achieve the specified CO_2 removal capacity.

3.1. **Effect of CO_2 removal rate**

The effect of the CO_2 removal rate on reboiler duty was first studied. As the removal rate increased from 50% to 90%, keeping the lean loading constant, the lean solvent flow rate was changed to reach the corresponding rate. The blend solvent was 28 wt% AMP+17 wt % PZ. The effects of changing the CO_2 removal rate on the rich loading and on the L/G ratio are presented in

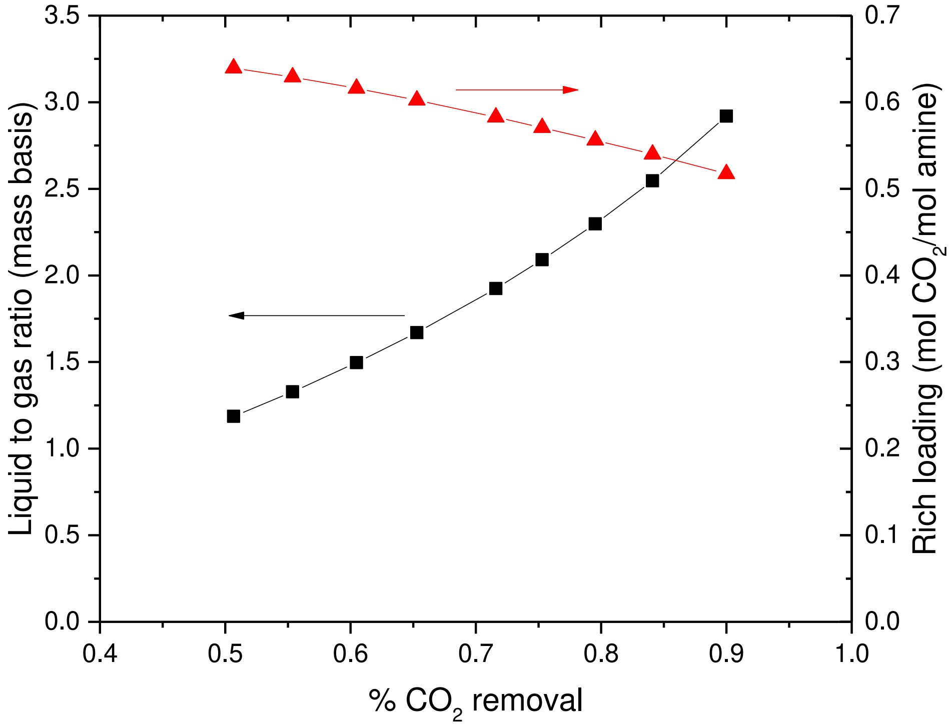

Figure 2**Error! Reference source not found.**. The rich loading decreases with increasing mass flow rate of the removed CO_2, implying that the required regeneration heat would also decrease to reach the same lean loading. However, to reach a higher removal capacity, more lean solvent is required as the lean loading remains unchanged, thus adding more solvent to be heated in the reboiler. As a result of the two factors, increasing the CO_2 removal rate produces a small increase in the reboiler duty (

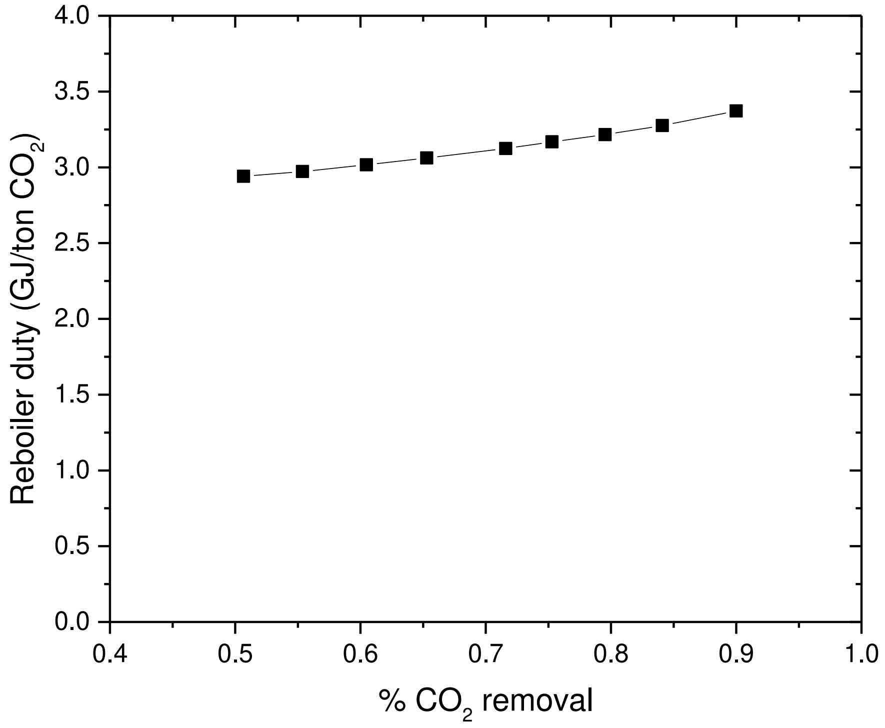

Figure 3**Error! Reference source not found.**).

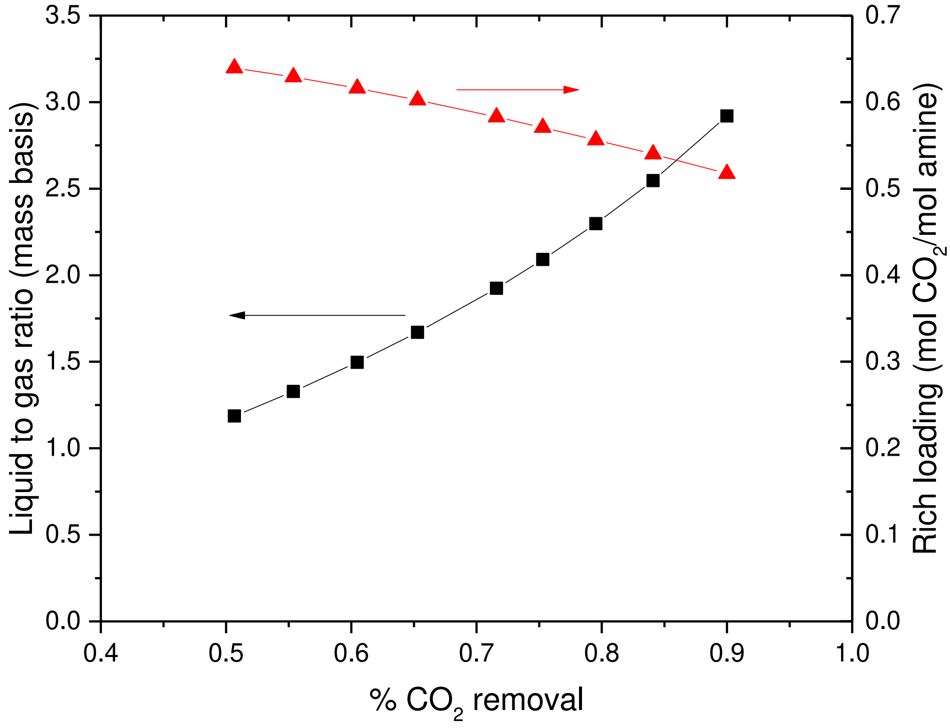

Figure 2. The effect of CO_2 removal rate on the L/G ratio and the rich loading (28 wt% AMP + 17 wt% PZ, lean loading=0.2 mol CO_2/mol amine).

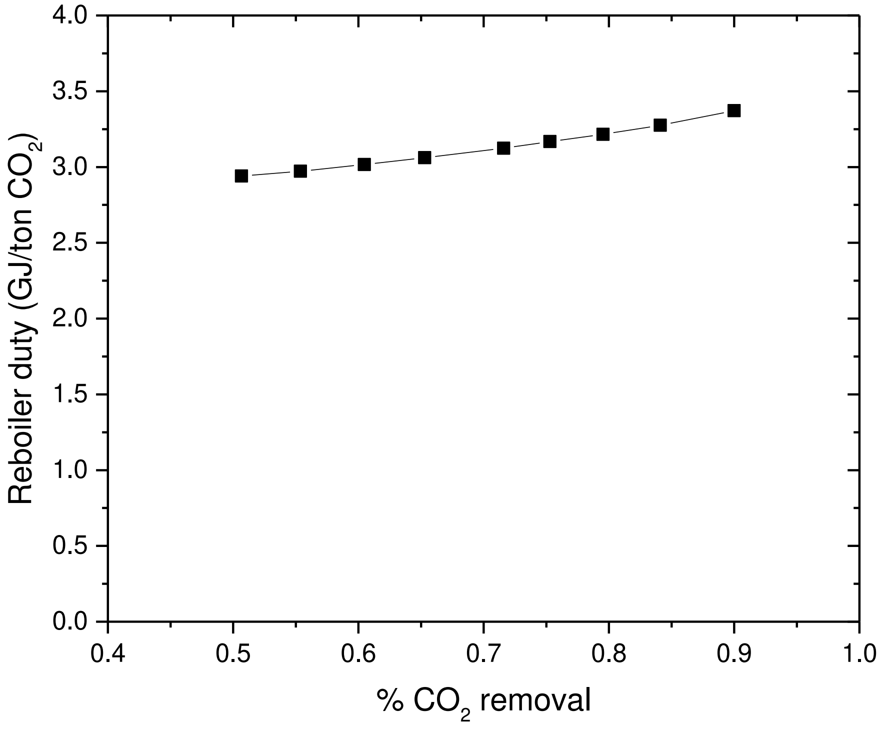

Figure 3. The effect of CO_2 removal rate on the reboiler duty (28 wt% AMP + 17 wt% PZ, lean loading=0.2 mol CO_2/mol amine).

3.2. **Effect of solvent composition**

The various compositions of the blend solvent were considered in different fixed L/G ratios at a removal rate of 90%. While varying the relative AMP and PZ concentrations, the total amine concentration in the aqueous solution was maintained at 45 wt%. Four kinds of compositions, 38 wt% AMP+7 wt% PZ, 33 wt% AMP+ 12 wt% PZ, 28 wt% AMP+17 wt% PZ, and 23 wt% AMP+22 wt% PZ , were studied for four fixed L/G ratios.

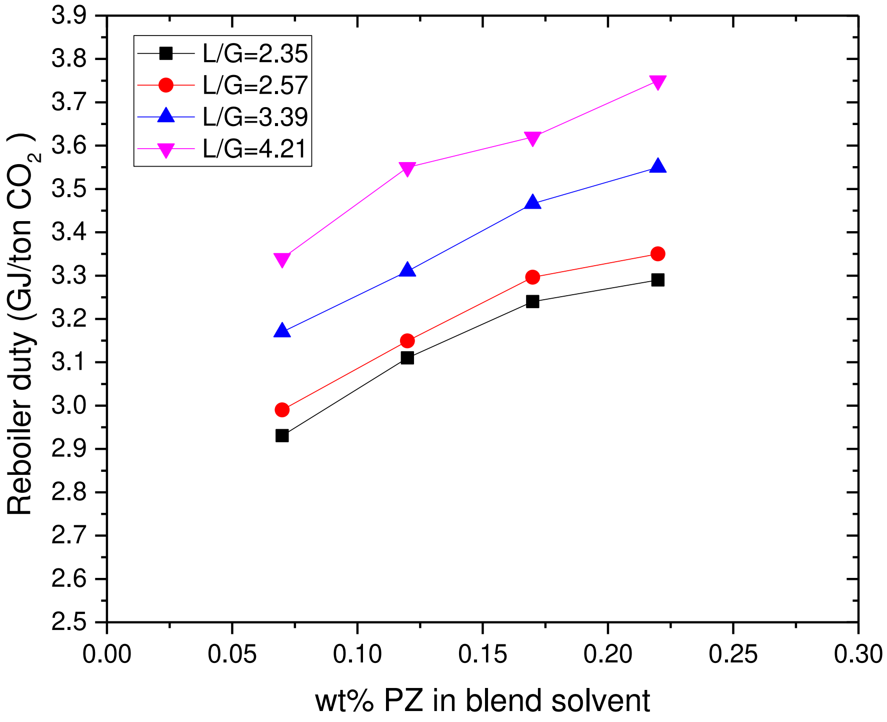

Figure 4**Error! Reference source not found.** shows that the reboiler duty increases with increasing PZ concentration.

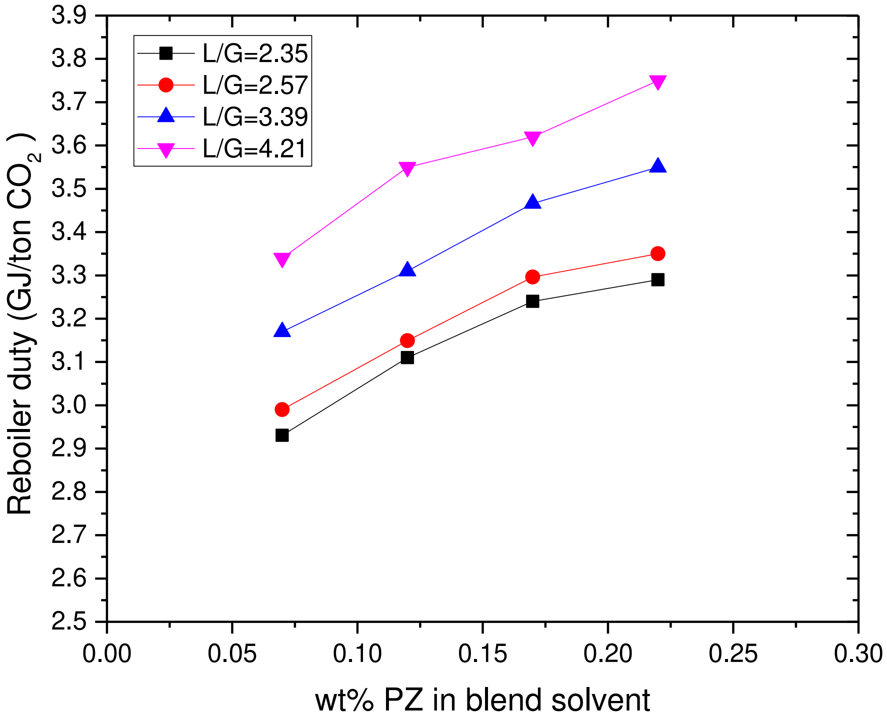

Figure 4. The effect of solvent composition on the reboiler duty (90% CO_2 removal rate, 4 fixed L/G ratios).

3.3. **Effect of CO_2 L/G ratio**

To study the performance of the full-scale CO_2 capture process, the L/G ratio was further optimized for each solvent composition to maintain a minimum regeneration heat, an essential parameter in solvent evaluation and selection. The condition of the flue gas remained unchanged.

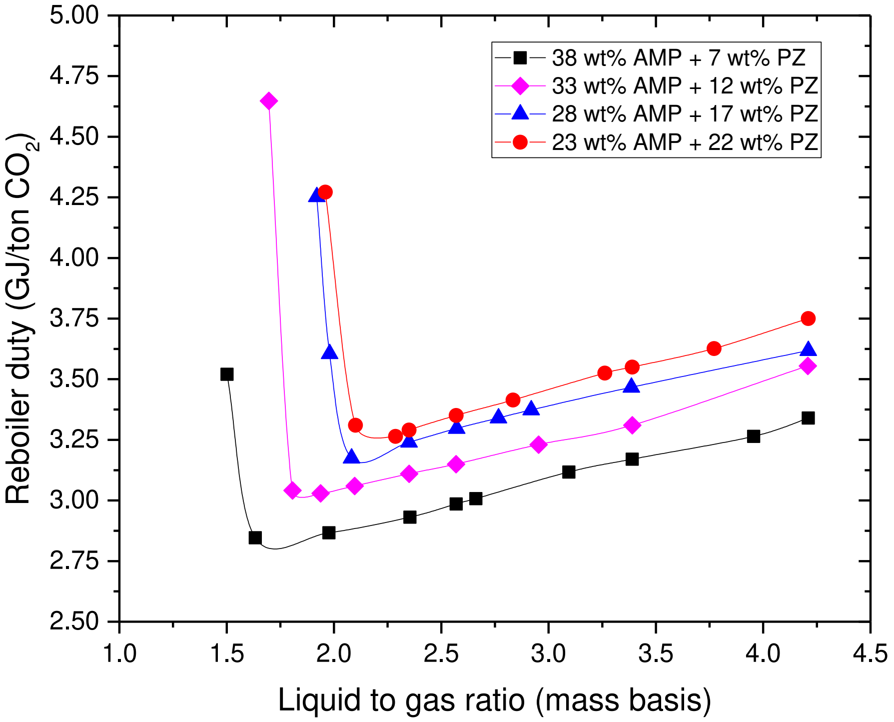

Figure 5**Error! Reference source not found.** compares the effect of the L/G ratio on the reboiler duty for the four different compositions. It could be seen that for each solvent, the reboiler duty first decreased and then increased with increasing L/G ratio. Therefore, a minimum reboiler duty could be obtained at a fixed L/G ratio and Table 7 presents the minimum value of reboiler duty and the corresponding L/G ratio.

From the literatures, for industrial scale carbon capture with 30wt% MEA solvent, the range of L/G ratio is from 0.70 to 2.75 for gas fired power plant and is from 2.00 to 5.50 for coal-fired power plant whilst the range of reboiler duty is from 3.5 to 5.0 GJ/ton CO_2 (Agbonghae et al., 2014; Hanak et al., 2014; Luo and Wang, 2016; Mac Dowell and Shah, 2014). It should be noted that for the blend solvent of AMP+PZ, the minimum reboiler duty and the corresponding L/G ratio were both lower than the standard solvent MEA, indicating that the blend solvent would be a promising substitute for MEA.

For different solvent composition, it could be observed that the optimal reboiler duty and the L/G ratio both increase as the concentration of PZ increases. This trend is due to the CO_2 loading capacity of AMP being much higher than PZ, causing the regeneration heat to be much lower. However, there have been reports that a small amount of PZ is essential as the activator in the blend solvent to improve the reaction rate. Samanta (Samanta and Bandyopadhyay, 2009) studied the effect of PZ on the kinetics of CO_2 absorption in aqueous solutions of AMP. The addition of small amounts of PZ to an aqueous solution of AMP results in a significant improvement in the rates of absorption. Dubois (Dubois and Thomas, 2012) reported that a cyclical amine (PZ or piperazi-nyl-1,2-ethylamine (PZEA)) when added to N-methyldiethanolamine (MDEA) or AMP aqueous solutions can substantially increase the CO_2 absorption rates due to the activation phenomenon. Brúder (Brúder and Svendsen, 2012) presented the experimental results of initial solvent characterization for the EU project CESAR and found that 3M AMP + 2M PZ (28 wt% AMP + 17 wt% PZ) has the highest absorption rate while the kinetics of 4M AMP + 1M PZ (36 wt% AMP + 8 wt% PZ) are much slower due to the AMP. Therefore, a relatively low concentration of PZ is recommended to reduce the energy consumption, while maintaining the enhancement in absorption rate.

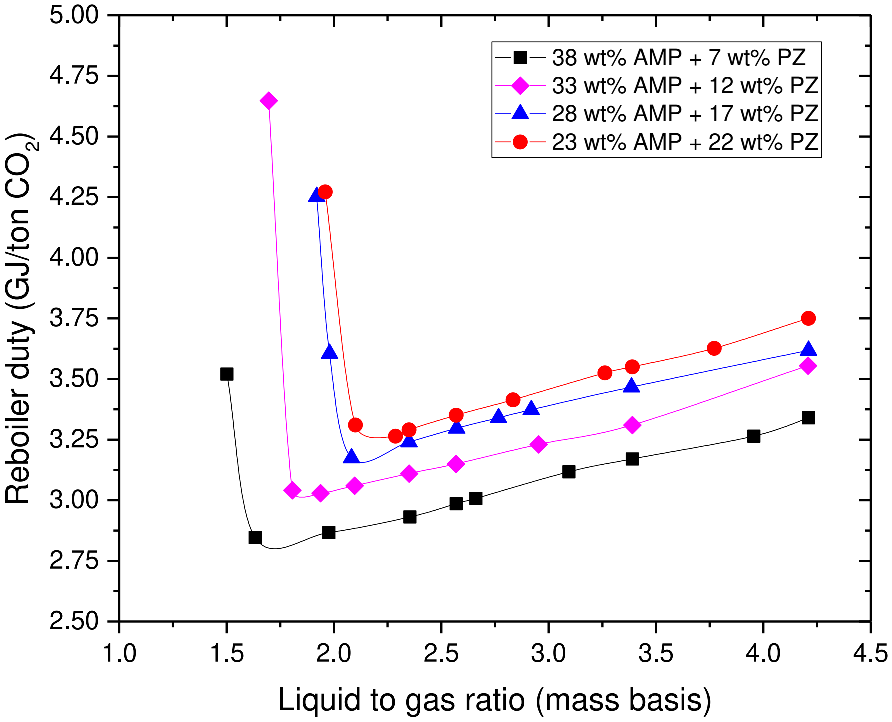

Figure 5. The effect of the L/G ratio on the reboiler duty for different solvent compositions (90% CO_2 removal rate, 4 fixed solvent compositions).

Table 7. Comparison of the optimal reboiler duty for different solvent compositions

Solvent composition	The optimal reboiler duty (GJ/ton CO_2)
38 wt% AMP+7 wt% PZ	2.84

33 wt% AMP+12 wt% PZ	3.02
28 wt% AMP+17 wt% PZ	3.18
23 wt% AMP+22 wt% PZ	3.25

3.4. **Effect of stripper pressure**

The effect of different stripper pressure conditions was also investigated. The stripper operating pressure was changed from 0.8 atm to 3 atm, assuming a total pressure drop of 0.2 atm in the column. The blend solvent was 0.28wt% AMP+0.17wt % PZ and the removal rate was fixed at 90%.

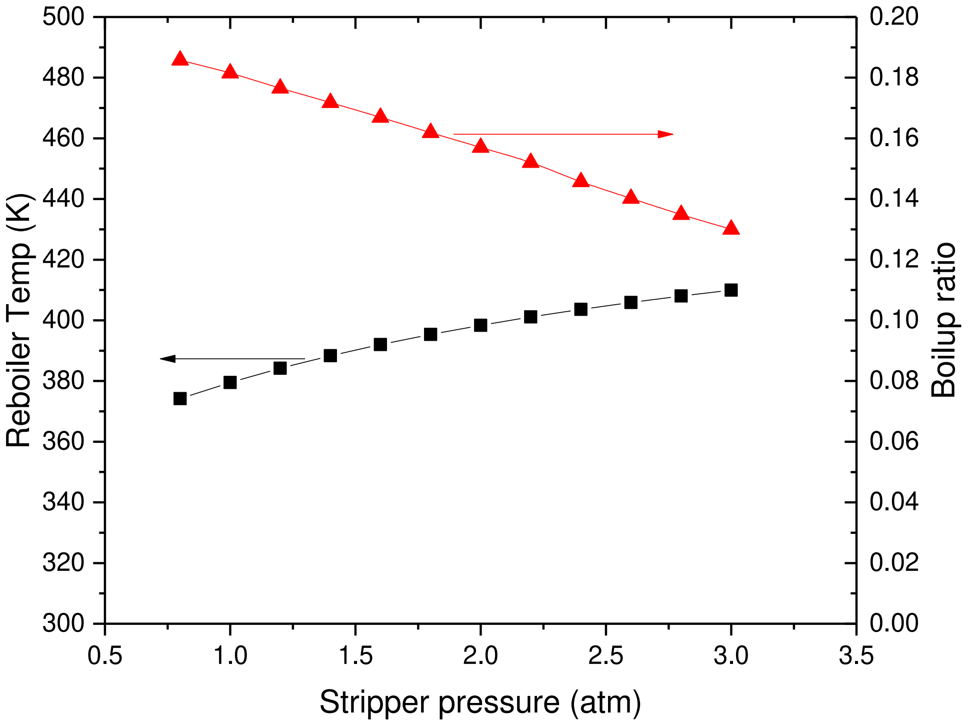

Figure 6**Error! Reference source not found.** shows the effect of stripper pressure on the reboiler temperature and on the boil up ratio. Clearly, a higher temperature could be reached at a higher pressure, where the CO_2 mass transfer rate and the reaction rate would be both improved and the boil up rate would decrease. However, the sensible heat required to bring the solvent to the reboiler temperature would also significantly increase, resulting in only a slight energy saving on reboiler duty, as presented in

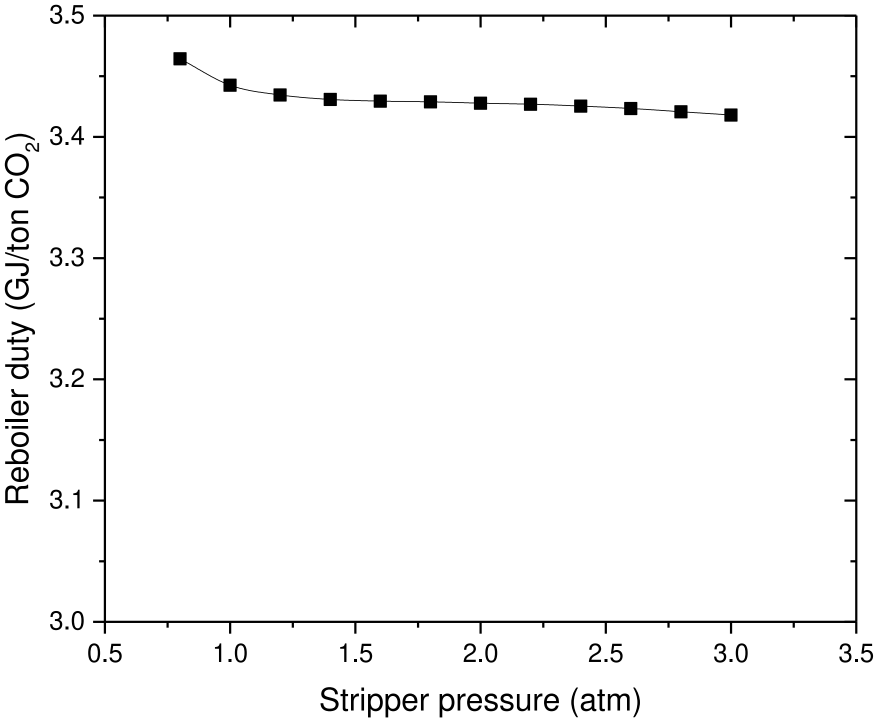

Figure 7**Error! Reference source not found.**. Considering higher amine degradation and corrosion problems at high temperatures and pressures, changing the stripper pressure to save energy might not be an economic way for optimizing this AMP+PZ blend solvent.

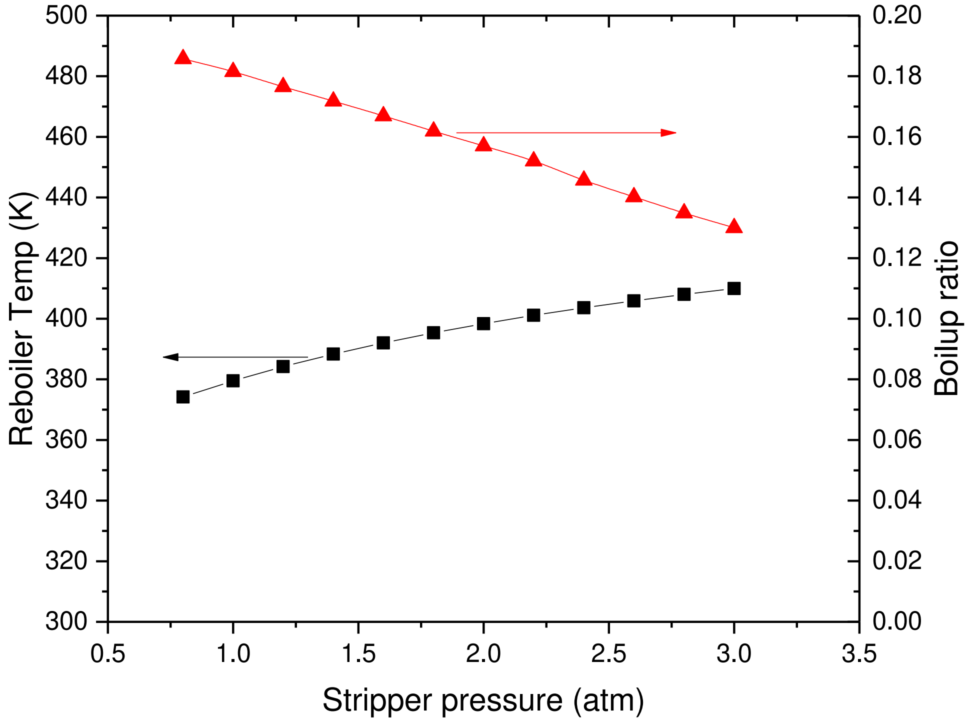

Figure 6. The effect of stripper pressure on the reboiler temperature and the boil up ratio (0.28wt% AMP+0.17wt % PZ, 90% CO_2 removal rate, L/G=2.12).

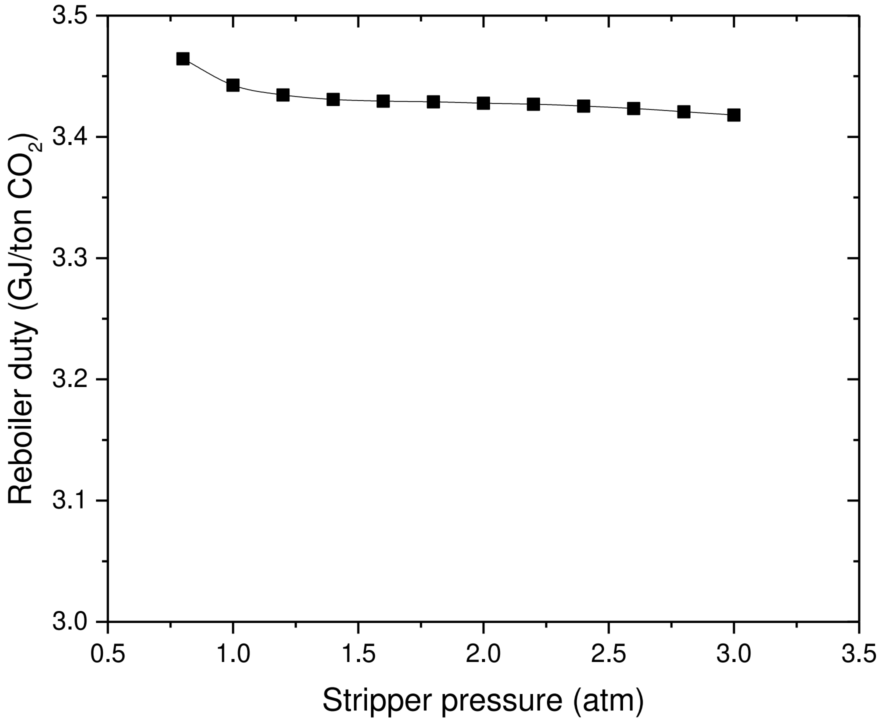

Figure 7. The effect of stripper pressure on the reboiler duty (0.28wt% AMP+0.17wt % PZ, 90% CO_2 removal rate, L/G=2.12).

4. **Process modification**

The energy consumption of CO_2 capture could also be reduced by incorporating process modifications into the standard process configuration (Xue et al., 2016). Therefore, the combination of novel solvent and an improved process was investigated in this work. Considering the pilot plant experiments of Knudsen (Knudsen et al., 2011) and other reported simulation results (Cousins et al., 2011; Le Moullec and Kanniche, 2011), three process modifications, intercooled absorber (ICA), lean vapor compressor (LVC), and rich solvent split (RSS), were chosen because they are most commonly used for CO_2 capture processes and have a proven high performances in energy saving.

Since there is additional electricity consumption in some process modifications, two types of energy should be considered: (i) mechanical energy for compressors and/or pumps and (ii) heat for the reboiler (Liang et al., 2015). These two should be unified because they exhibit different energy values so that a global comparison between different processes could be made. The equivalent work is used to evaluate the energy requirement of running the stripper and the additional compressors or pumps. The overall equivalent work is calculated using the following equation (Van Wagener and Rochelle, 2011).

$$W_{eq} = 0.75 \times Q_{reb} \left(\frac{T_i + 10K - T_{sink}}{T_i + 10K} \right) + W_{add} \tag{11}$$

where T_i is the reboiler temperature, the temperature of steam in the reboiler is 10 K higher than T_i, Q_{reb} is the reboiler duty, T_{sink} is is the cold end temperature of Carnot engine, and set at 313 K, and W_{add} is additional work (like compression work).

The electric penalty was calculated using a Carnot efficiency term, which accounted for the increasing value of steam at high temperature. Additionally, 75% efficiency was applied to account for non-ideal expansion in the steam turbines. Using the blend solvent of composition 28 wt% AMP+17 wt% PZ, the full-scale baseline case in Section 3 is used to investigate the energy reduction of each process modification, and the equivalent work of this base case is 0.533 GJ/ton CO_2.

4.1. **Intercooled absorber (ICA)**

The ICA is a well-known technique commonly applied by both researchers and industries. CO_2 absorption is an exothermic reaction, resulting in an overall temperature increase in the column, which limits the driving force for absorption and thereby lowers the absorption capacity of the solvent. Therefore, controlling the temperature of the absorber could be an efficient way to enhance CO_2 recovery and reduce the required solvent flow rate by enhancing the thermodynamic driving force. The flowsheet (Figure 8**Error! Reference source not found.**) (Cousins et al., 2011) illustrates that the principle of this modification is to withdraw a fraction or all of the liquid flow from the column at one of its stages, cool it down and then to send it back to the column. In this study, the whole liquid flow was removed from the absorber, pumped to 1.1 atm to prevent the pressure drop, cooled to 40 °C, and then re-injected back.

To evaluate the effect of the intercooling stage, the absorber was set at 20 stages, and the optimal result is shown in

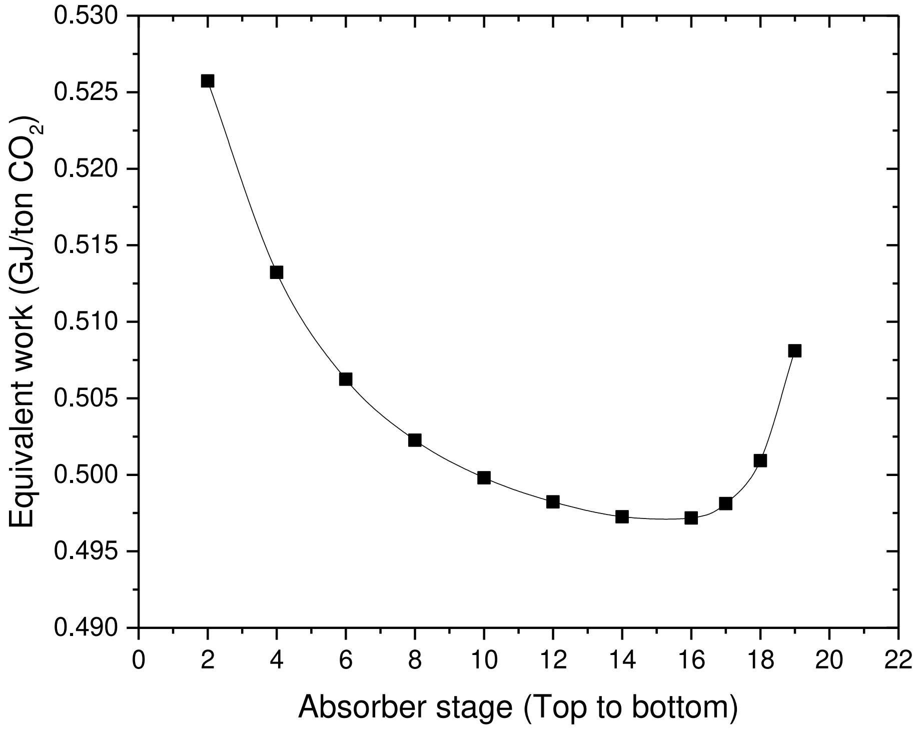

Figure 9. In the top of the column, the solvent was fresh with a rather low CO_2 loading; therefore, changing the temperature of the stream had a limited effect. In the lower part of

the column, where the CO_2 loading in the solvent and the temperature were both higher, cooling the solvent would significantly increase the driving force. At the bottom, however, the CO_2 loading reaches a rather high level, where the driving force is hardly enhanced by changing the temperature. Consequently, the minimum equivalent work of 0.497 GJ/ton CO_2, which translates to a 6.7% energy saving compared to the base case, is obtained in stage 16.

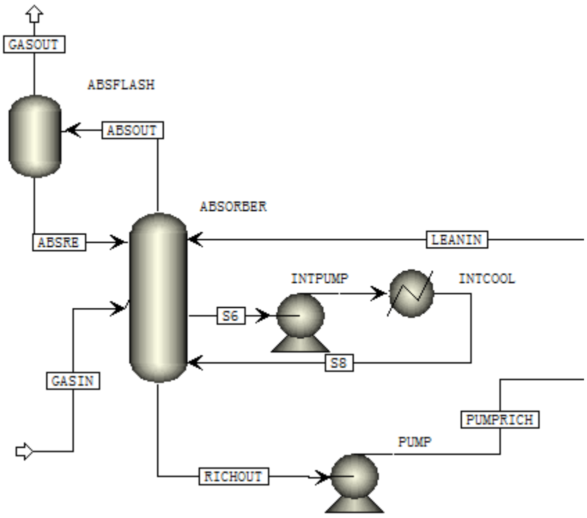

Figure 8. Flowsheet (modified part) of the intercooled absorber.

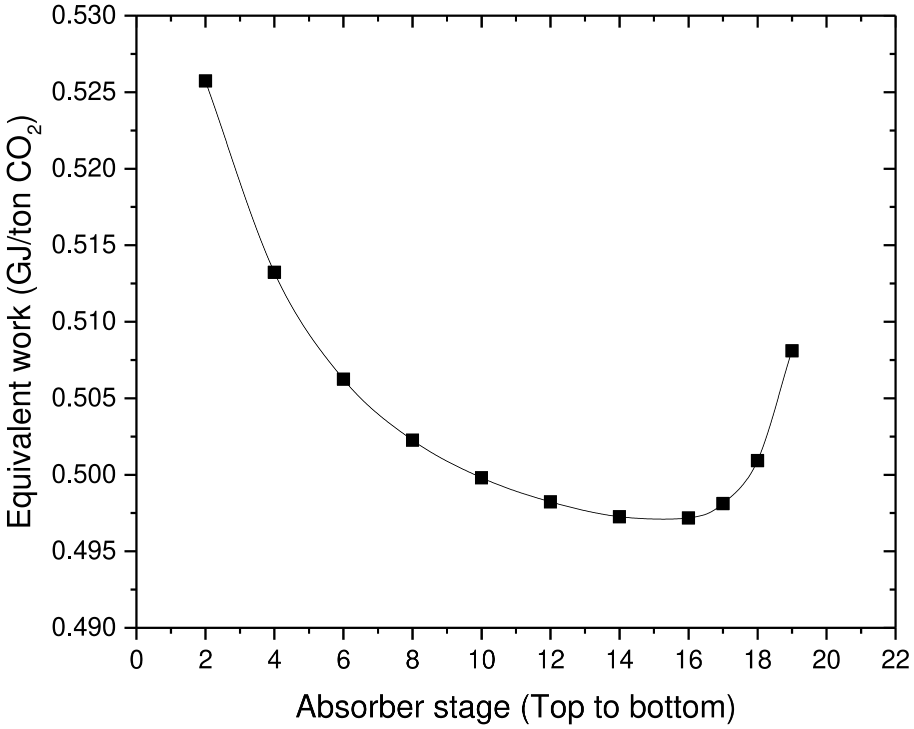

Figure 9. The effect of intercooling stage on the equivalent work.

4.2. **Lean vapor compressor (LVC)**

In LVC schemes, the hot lean solvent leaving the bottom of the stripper was flashed to produce a gaseous stream, which was then compressed and fed back to the stripper. The flowsheet of this modification (Figure 10**Error! Reference source not found.**) is the same as in the patent of Batteux (Batteux and Godard, 1983). Benefitting from the sensible heat of hot lean solvent as well as recompression, the compressed vapor stream could reach a very high temperature, producing additional steam and heat for the stripper. However, although the reboiler duty was reduced, there was additional electricity consumption when a compressor was introduced. In this study, the adiabatic efficiency of the compressor was modeled as 80%, and the equivalent work was equal to the sum of the reboiler duty and the additional work of the compressor.

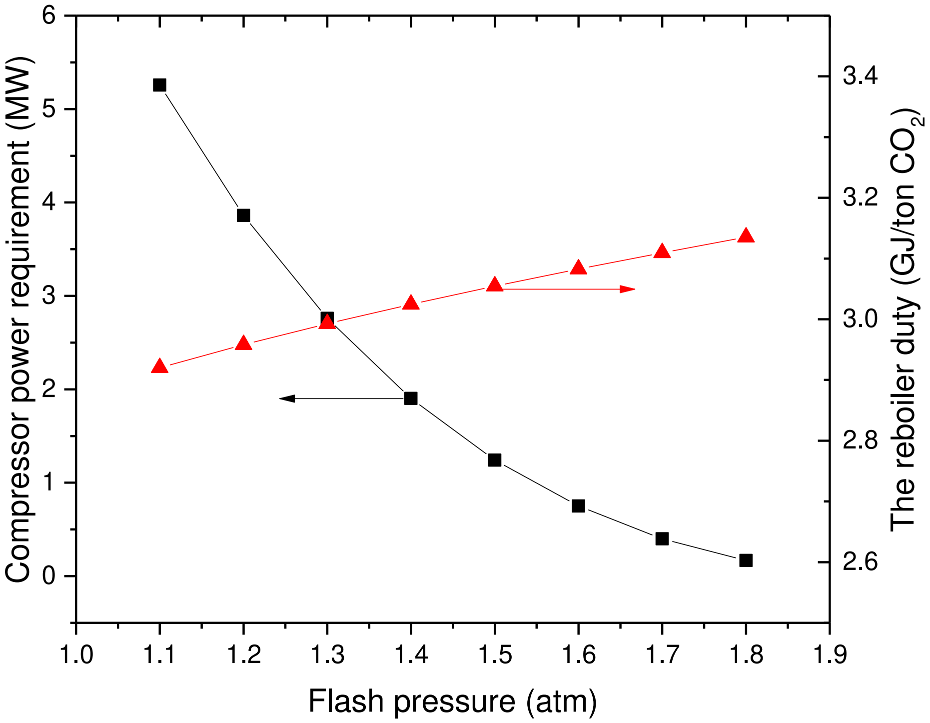

Figure 11**Error! Reference source not found.** shows the effect of flash pressure on the power requirement of the compressor and on the reboiler duty. The power requirement increased and reboiler duty decreased with decreasing flash pressure. Hence, there was an optimal flash pressure for the minimum total equivalent work, which is a sum of those two parts, as presented in

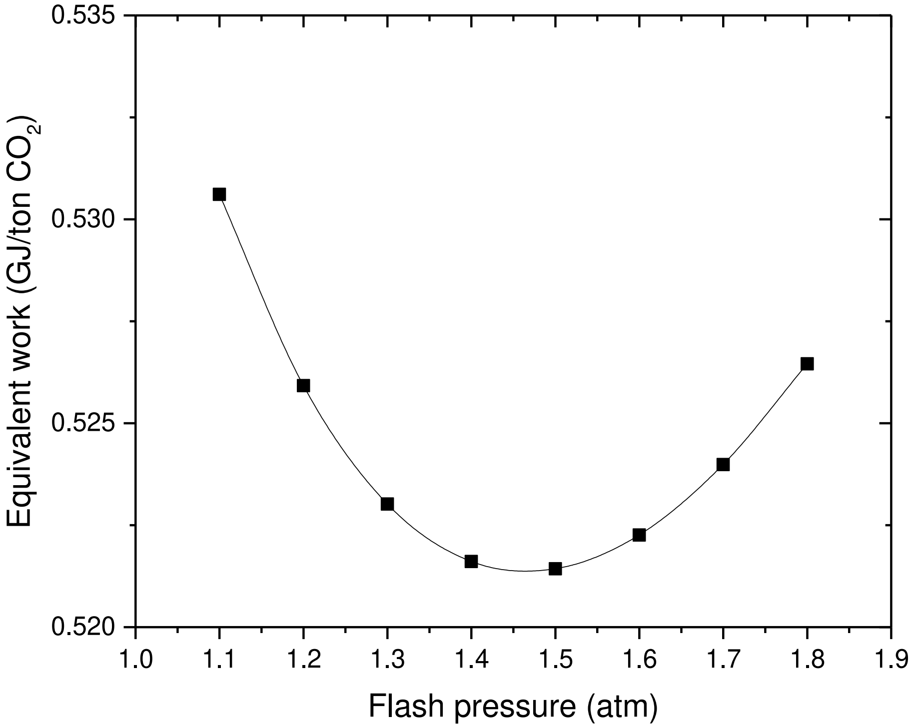

Figure 12**Error! Reference source not found.**. The final pressure of the re-injected gas stream should be consistent with the reboiler pressure. Lowering the initial flash pressure would lead to a temperature increase of the compressed vapor, which would provide additional stripping steam and heat. However, as additional work of the compressor increases, a larger amount of vapor should be compressed (Figure 13). Compared to the base case, a minimum equivalent work of 0.521 GJ/ton CO_2 was obtained at a flash pressure of 1.5 atm, giving a total energy saving of ~2.7%.

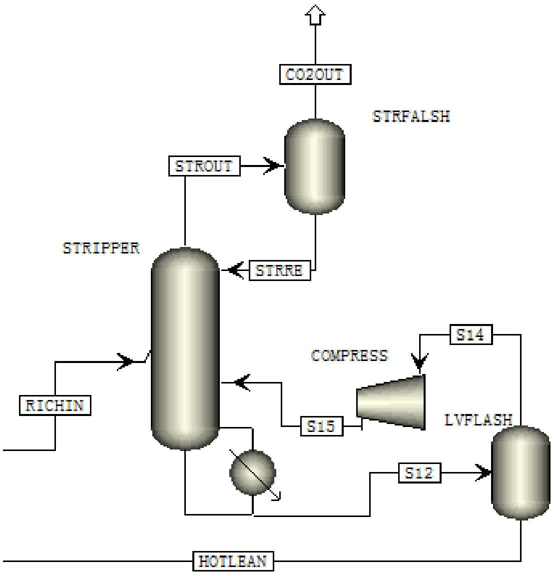

Figure 10. Flowsheet (modified part) of the lean vapor compressor.

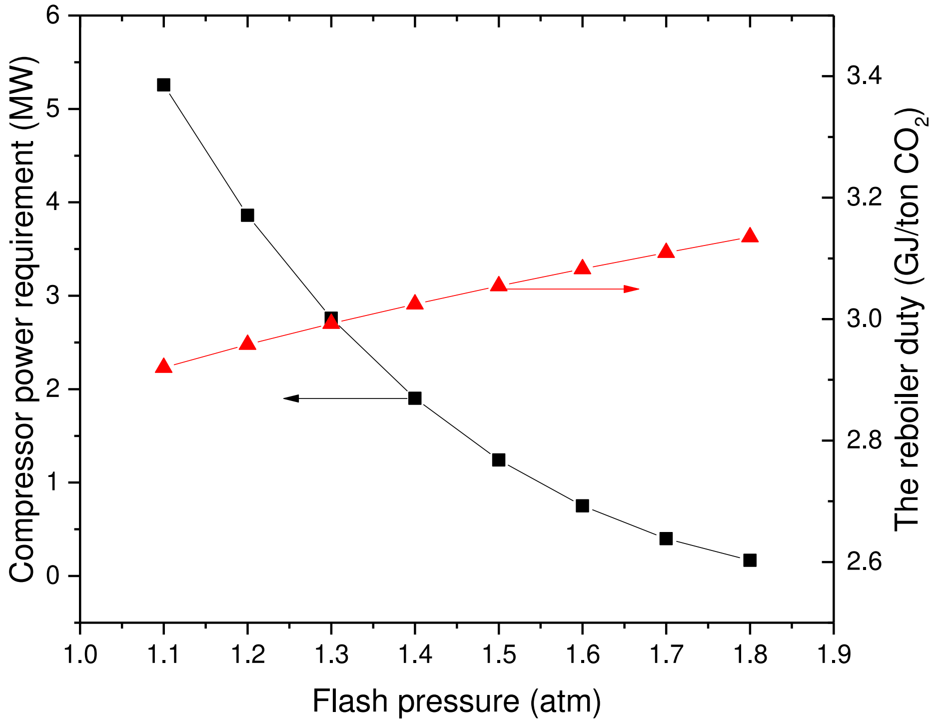

Figure 11. The effect of flash pressure on compressor power requirement and reboiler duty.

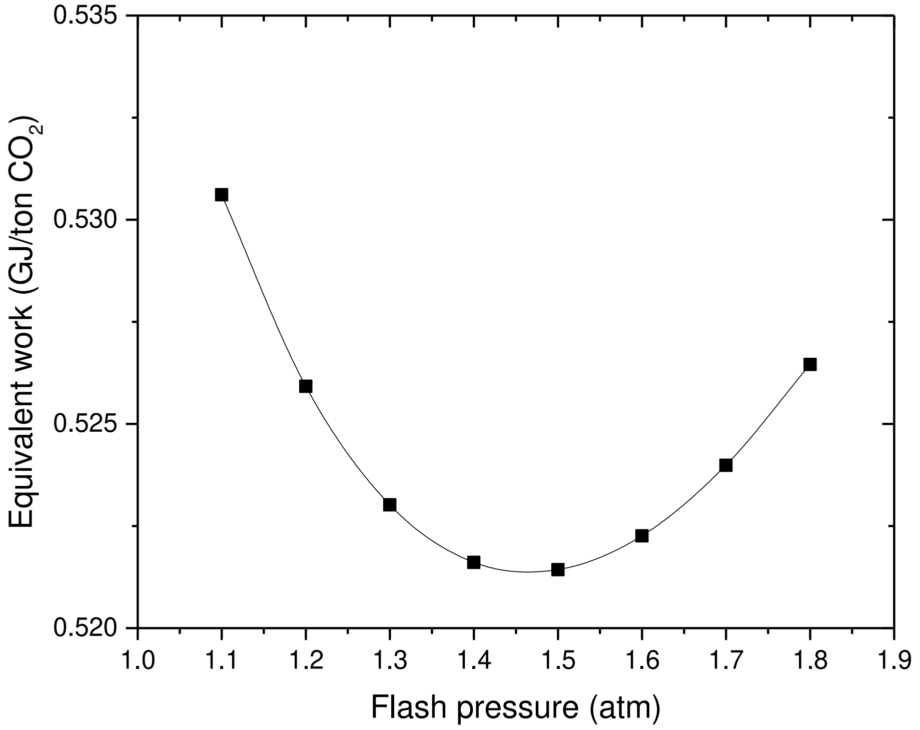

Figure 12. The effect of flash pressure on the equivalent work.

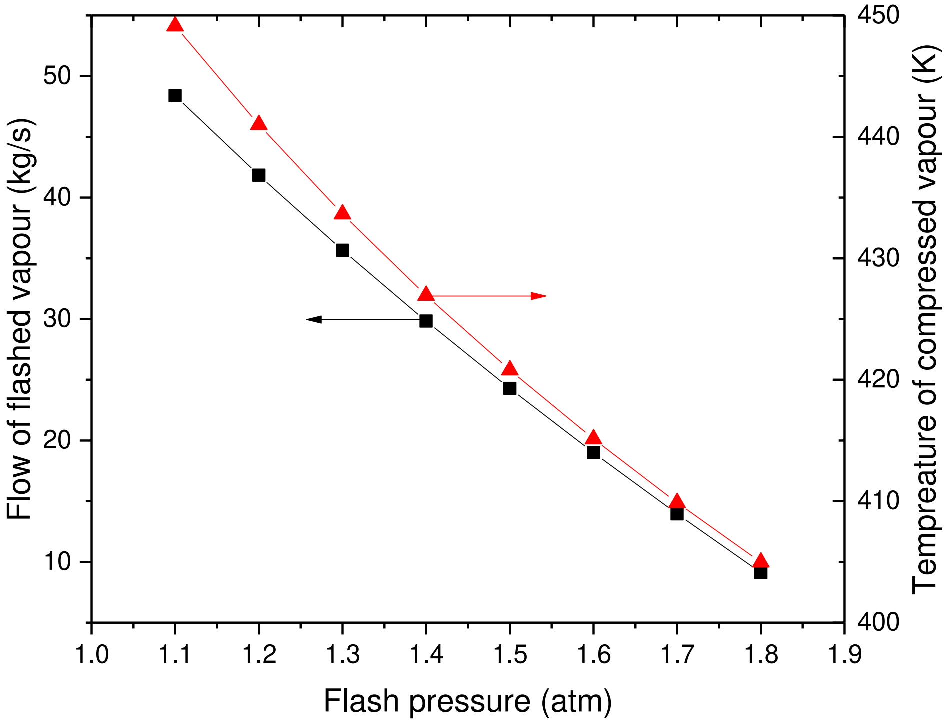

Figure 13. The effect of flash pressure on flow and temperature of compressed vapor.

4.3. **Rich solvent split (RSS)**

This simple modification (Figure 14**Error! Reference source not found.**) involved splitting the rich stream into two flows: one directly entering the top of stripper remaining unheated and one heated in the lean/rich heat exchanger and then injected into the column at a distance below the top, as suggested by the patent of Eisenberg (Eisenberg and Johnson, 1979). With this modification, the heated portion of the solvent flow reaches a higher temperature, which was favorable for desorption reactions. The re-injection of the hot stream in the middle of the stripper also allowed pre-stripping of the cold rich solvent that flowed down the top of the stripping column. The entering stage of heated rich solvent was optimized (from stage 2 to 6) and stage 3 was found to be the optimal stage to maintain the minimum reboiler duty.

The split fraction (the fraction of the un-heated stream to the initial rich solvent) was then varied to find an optimal energy saving. Up to 70% fraction reduced the reboiler duty compared to the base case, as shown in

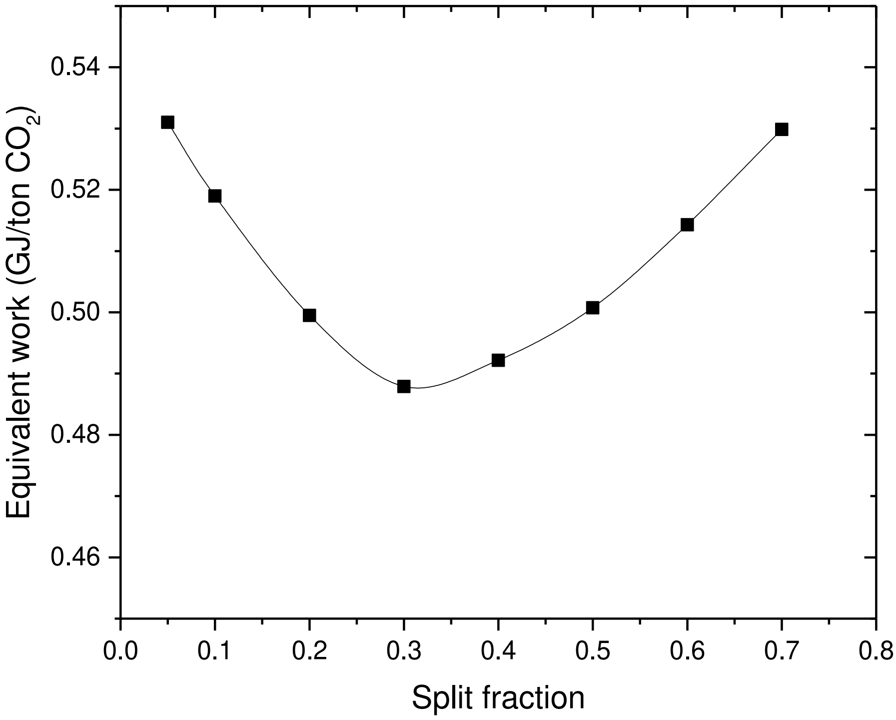

Figure 15. It should be noted that when the fraction increased, the reboiler was required to provide more heat for the cold stream. Meanwhile, in the lean/rich heat exchanger, the heat of the hot lean solvent might be wasted if the cold rich solvent was not sufficient. The temperature of the stripping vapor first increased and then decreased with increasing split fraction

(

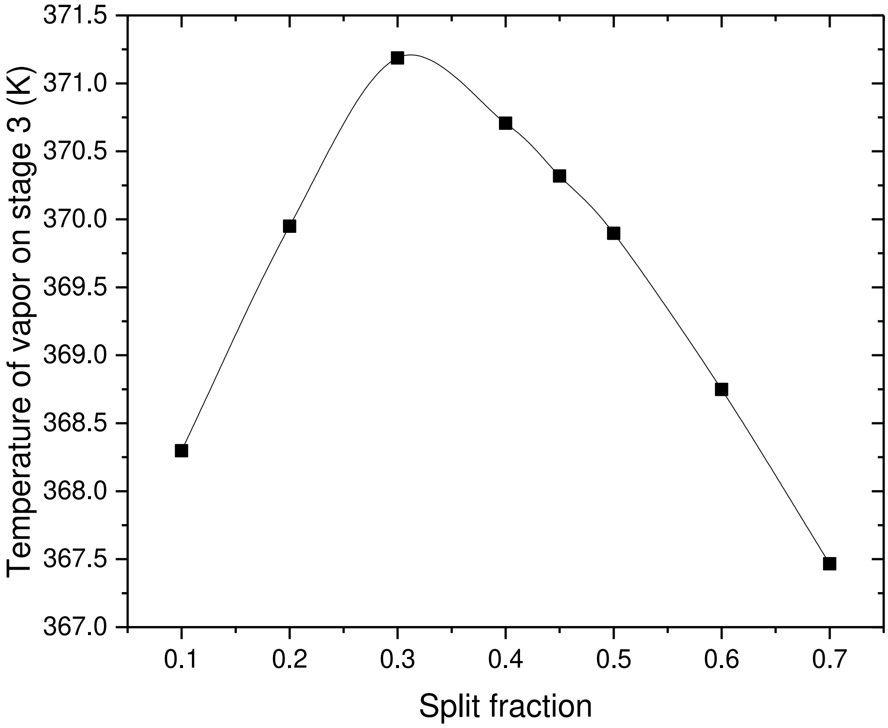

Figure 16**Error! Reference source not found.**). At a split fraction of 0.3, the stripping vapor reached the highest temperature, implying that a maximum utilization of heat was obtained. The optimal equivalent work was 0.488 GJ/ton CO_2, giving an 8.5% energy saving compared to the base case.

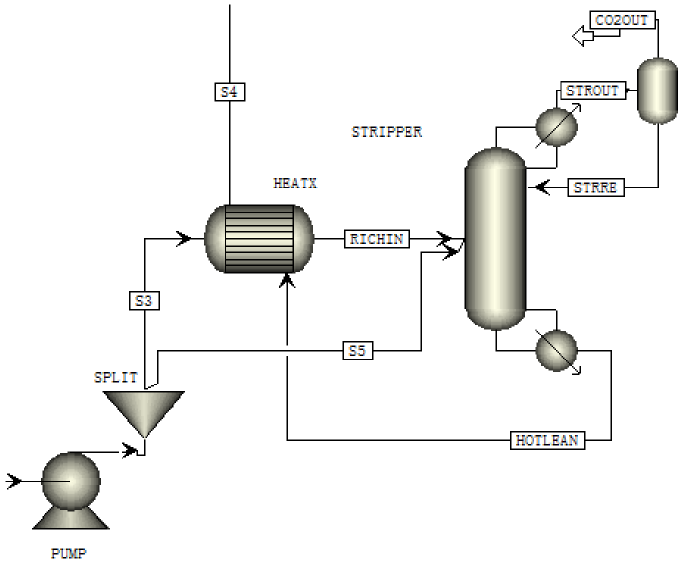

Figure 14. Flowsheet (modified part) of the rich solvent split.

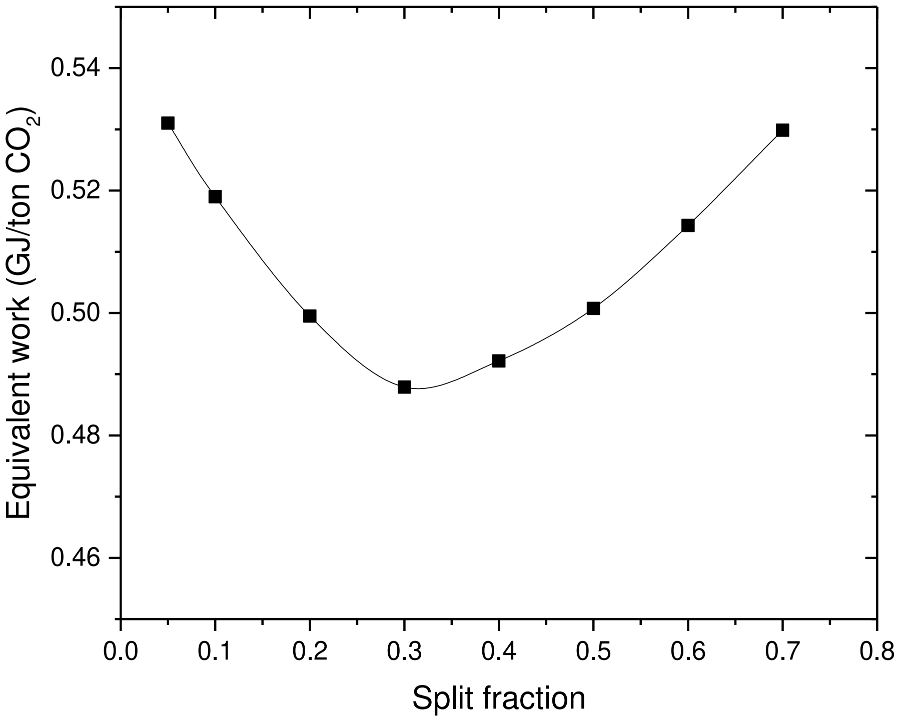

Figure 15. The effect of split fraction on the equivalent work.

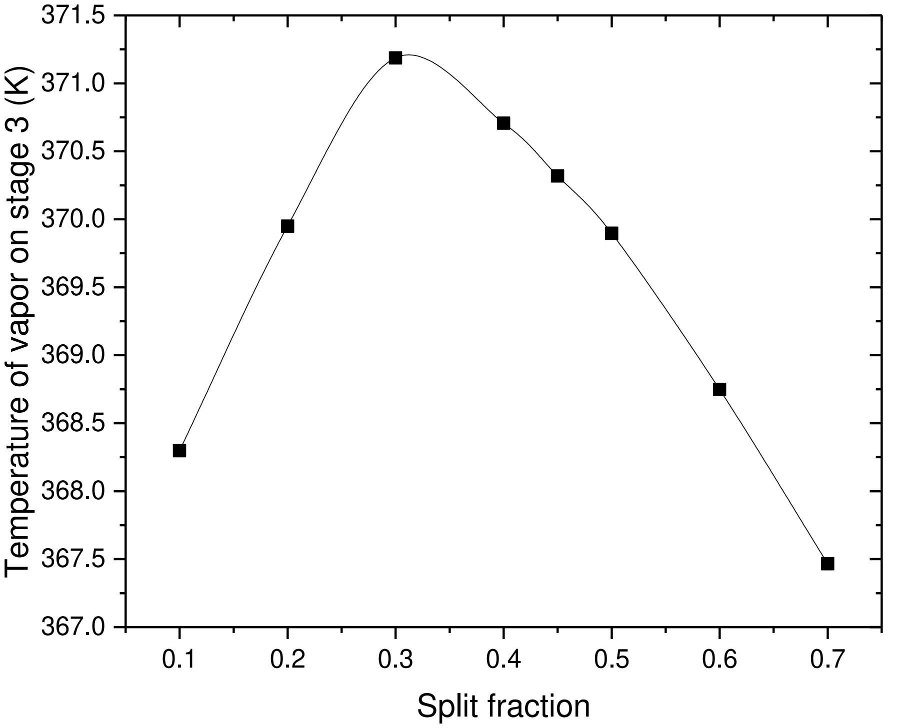

Figure 16. The effect of split fraction on the temperature of the stripping vapor.

4.4. **Combination of process modifications**

A combination of process modifications could lead to a further significant reduction in energy consumption. In this study, ICA was a modification of the absorber that enhanced the absorption process by increasing the thermodynamic driving force. LVC was a modification of the stripper resulting in benefits from the sensible heat of hot lean solvent and recompression. With the intercooling stage of stage 16 and the flash pressure of 1.4 atm (which are both optimal specifications), the simulation result of this optimal configuration shows an 8.5% energy saving in equivalent work.

RSS is also a different stripper configuration that takes advantage of heat integration. With the intercooling stage of stage 16 and the split fraction of 0.3, the combination reduces the equivalent work by 14%. The combination of RSS and LVC could further reduce the equivalent work. With the split fraction of 0.3 and the flash pressure of 1.7 atm, the optimized equivalent work savings was 9.3%. The combination of all three kinds of process modifications could reduce the equivalent work by 15.2%, indicating that the combination of process modifications could further enhance energy savings.

5. **Conclusion**

In this paper, a modeling and process analysis study of a blend solvent AMP+PZ for CO_2 capture process was presented. An rate-based model based on the absorption–regeneration process was developed in Aspen Plus® and validated with pilot plant experimental data. The validated model was scaled-up and optimized to handle the flue gas from a 600-MW_e coal-fired power plant.

The full-scale model was then used to study the effects of CO_2 removal rate, solvent composition, and stripper pressure on the energy requirement. It was observed that the reboiler duty would be reduced when lowering the CO_2 removal rate, increasing the ratio of AMP in the solvent and increasing the stripper pressure. For a fixed removal rate and solvent composition, the reboiler duty first decreased as the L/G ratio increased and then increased as the L/G ratio increased. The lowest reboiler duty of 3.18 GJ/ton CO_2 could be achieved with 90% CO_2 removal, 28 wt% AMP+17 wt% PZ solvent, and an L/G ratio of 2.1.

Furthermore, process configuration modifications to the standard process have been implemented to reduce the energy demand. ICA, LVC and RSS were therefore simulated using the scale-up process model. The equivalent work was considered to compare the total energy consumption. A reduction of 6.7%, 2.7%, and 8.5% in energy demand was obtained by ICA, LVC and RSS modifications separately. The combination of ICA+LVC, ICA+RSS, and RSS+LVC modifications obtained a further energy saving of 8.5%, 14%, and 9.3% respectively. The combination of ICA +RSS+LVC reduced the energy demand by 15.2%.

References

Agbonghae, E.O., Hughes, K.J., Ingham, D.B., Ma, L., Pourkashanian, M., 2014. Optimal process design of commercial-scale amine-based CO2 capture plants. Ind. Eng. Chem. Res. 53, 14815–14829. doi:10.1021/ie5023767

Artanto, Y., Jansen, J., Pearson, P., Puxty, G., Cottrell, A., Meuleman, E., Feron, P., 2014. Pilot-scale evaluation of AMP/PZ to capture CO2 from flue gas of an Australian brown coal-fired power station. Int. J. Greenh. Gas Control 20, 189–195. doi:10.1016/j.ijggc.2013.11.002

Batteux, J., Godard, A., 1983. Process and installation for regenerating an absorbent solution containing gaseous compounds.

Bavbek, O., Alper, E., 1999. Reaction Mechanism and Kinetics of Aqueous Solutions of Primary and Secondary Alkanolamines and Carbon Dioxide. Turk. J. Chem. 23, 293–300.

Bishnoi, S., Rochelle, G.T., 2002. Absorption of carbon dioxide in aqueous piperazine/methyldiethanolamine. AIChE J. 48, 2788–2799. doi:10.1002/aic.690481208

Bishnoi, S., Rochelle, G.T., 2000. Absorption of carbon dioxide into aqueous piperazine: reaction kinetics, mass transfer and solubility. Chem. Eng. Sci. 55, 5531–5543. doi:10.1016/S0009-2509(00)00182-2

Brúder, P., Svendsen, H.F., 2012. Capacity and kinetics of solvents for post-combustion CO 2 capture 23, 45–54. doi:10.1016/j.egypro.2012.06.028

Brúder, P., Grimstvedt, A., Mejdell, T., Svendsen, H.F., 2011. CO2 capture into aqueous solutions of piperazine activated 2-amino-2-methyl-1-propanol. Chem. Eng. Sci. 66, 6193–6198. doi:10.1016/j.ces.2011.08.051

Brúder, P., Grimstvedt, A., Mejdell, T., Silva, F., 2010. CO 2 capture into aqueous solutions of the mixed solvent Cesar 1, Proceedings of the 2nd Annual Gas Processing Symposium. Elsevier B.V. doi:10.1016/S1876-0147(10)02004-5

Chowdhury, F.A., Okabe, H., Yamada, H., Onoda, M., Fujioka, Y., 2011. Synthesis and selection of hindered new amine absorbents for CO2 capture. Energy Procedia 4, 201–208. doi:10.1016/j.egypro.2011.01.042

Cousins, A., Wardhaugh, L.T., Feron, P.H.M., 2011. Preliminary analysis of process flow sheet modifications for energy efficient CO2 capture from flue gases using chemical absorption. Chem. Eng. Res. Des. 89, 1237–1251. doi:10.1016/j.cherd.2011.02.008

Dash, S.K., Samanta, A., Nath Samanta, A., Bandyopadhyay, S.S., 2011. Absorption of carbon dioxide in piperazine activated concentrated aqueous 2-amino-2-methyl-1-propanol solvent. Chem. Eng. Sci. 66, 3223–3233. doi:10.1016/j.ces.2011.02.028

Dash, S.K., Samanta, A.N., Bandyopadhyay, S.S., 2014. Simulation and parametric study of post combustion CO2 capture process using (AMP+PZ) blended solvent. Int. J. Greenh. Gas Control 21, 130–139. doi:10.1016/j.ijggc.2013.12.003

Dubois, L., Thomas, D., 2012. Screening of Aqueous Amine-Based Solvents for Postcombustion CO 2 Capture by Chemical Absorption. Chem. Eng. Technol. 35, 513–524. doi:10.1002/ceat.201100523

Eisenberg, B., Johnson, R.R., 1979. Amine regeneration process.

Freeman, S.A., Davis, J., Rochelle, G.T., 2010a. Degradation of aqueous piperazine in carbon dioxide capture. Int. J. Greenh. Gas Control 4, 756–761. doi:10.1016/j.ijggc.2010.03.009

Freeman, S.A., Dugas, R., Van Wagener, D.H., Nguyen, T., Rochelle, G.T., 2010b. Carbon dioxide capture with concentrated, aqueous piperazine. Int. J. Greenh. Gas Control 4, 119–124. doi:10.1016/j.ijggc.2009.10.008

Freguia, S., Rochelle, G.T., 2003. Modeling of CO2 capture by aqueous monoethanolamine. AIChE J. 49, 1676–1686.

Hanak, D.P., Biliyok, C., Yeung, H., Bia??ecki, R., 2014. Heat integration and exergy analysis for a supercritical high-ash coal-fired power plant integrated with a post-combustion carbon capture process. Fuel 134, 126–139. doi:10.1016/j.fuel.2014.05.036

Knudsen, J.N., Andersen, J., Jensen, J.N., Biede, O., 2011. Results from test campaigns at the 1 t/h CO2 post-combustion capture pilot-plant in Esbjerg under the EU FP7 CESAR project. 1st Post Combust. Capture Conf. 2–3.

Le Moullec, Y., Kanniche, M., 2011. Screening of flowsheet modifications for an efficient monoethanolamine (MEA) based post-combustion CO2 capture. Int. J. Greenh. Gas Control 5, 727–740. doi:10.1016/j.ijggc.2011.03.004

Lepaumier, H., Picq, D., Carrette, P.L., 2009. New amines for CO2 Capture. II. oxidative degradation mechanisms. Ind. Eng. Chem. Res. 48, 9068–9075. doi:10.1021/ie9004749

Li, H., Frailie, P.T., Rochelle, G.T., Chen, J., 2014. Thermodynamic modeling of piperazine/2-aminomethylpropanol/CO2/water. Chem. Eng. Sci. 117, 331–341. doi:10.1016/j.ces.2014.06.026

Liang, Z., Gao, H., Rongwong, W., Na, Y., 2015. Comparative studies of stripper overhead vapor integration-based configurations for post-combustion CO2 capture. Int. J. Greenh. Gas Control 34, 75–84. doi:10.1016/j.ijggc.2014.12.019

Mac Dowell, N., Shah, N., 2014. Dynamic modelling and analysis of a coal-fired power plant integrated with a novel split-flow configuration post-combustion CO2 capture process. Int. J. Greenh. Gas Control 27, 103–119. doi:10.1016/j.ijggc.2014.05.007

Mangalapally, H.P., Hasse, H., 2011a. Pilot plant experiments for post combustion carbon dioxide capture by reactive absorption with novel solvents. Energy Procedia 4, 1–8. doi:10.1016/j.egypro.2011.01.015

Mangalapally, H.P., Hasse, H., 2011b. Pilot plant study of two new solvents for post combustion carbon dioxide capture by reactive absorption and comparison to monoethanolamine. Chem. Eng. Sci. 205–216. doi:10.1016/j.ijggc.2012.02.014

Niu, Z., Guo, Y., Zeng, Q., Lin, W., 2012. Experimental studies and rate-based process simulations of CO2 absorption with aqueous ammonia solutions. Ind. Eng. Chem. Res. 51, 5309–5319. doi:10.1021/ie2030536

Pinsent, B.R.W., Pearson, L., Roughton, F.J.W., 1956. The kinetics of combination of carbon dioxide with hydroxide ions. Trans. Faraday Soc. 52, 1512–1520. doi:10.1039/TF9565201512

Saha, A.K., Bandyopadhyay, S.S., Biswas, A.K., 1995. Kinetics of absorption of CO2 into aqueous solutions of 2-amino-2-methyl-1-propanol. Chem. Eng. Sci. 50, 3587–3598. doi:10.1016/0009-2509(95)00187-A

Samanta, A., Bandyopadhyay, S.S., 2009. Absorption of carbon dioxide into aqueous solutions of piperazine activated 2-amino-2-methyl-1-propanol. Chem. Eng. Sci. 64, 1185–1194. doi:10.1016/j.ces.2008.10.049

Sinnott, R., Towler, G., 2013. Chapter 17 – Separation Columns (Distillation, Absorption, and Extraction), in: Chemical Engineering Design – Principles, Practice and Economics of Plant and Process Design. pp. 807–935. doi:10.1016/B978-0-08-096659-5.00017-1

Śpiewak, D., Krótki, A., Spietz, T., Stec, M., Więcław–Solny, L., Tatarczuk, A., Wilk, A., 2015. PDU-Scale Experimental Results of CO2 Removal With Amp/Pz Solvent. Chem. Process Eng. 36, 39–48. doi:10.1515/cpe-2015-0003

Taylor, R., Krishna, R., Kooijman, H., 2003. Real-world modeling of distillation. Chem. Eng. Prog. 99, 28–39.

Van Wagener, D.H., Rochelle, G.T., 2011. Stripper configurations for CO2 capture by aqueous monoethanolamine. Chem. Eng. Res. Des. 89, 1639–1646. doi:10.1016/j.cherd.2010.11.011

Zhang, Y., Chen, H., Chen, C.C., Plaza, J.M., Dugas, R., Rochelle, G.T., 2009. Rate-based process modeling study of CO2 Capture with aqueous monoethanolamine solution. Ind. Eng. Chem. Res. 48, 9233–9246. doi:10.1021/ie900068k